NONLINEAR FINITE ELEMEN ANALYSIS OF HIGH STREGTH REINFORCED CONCRETE SLABS

Dr. Ihsan A. S. Al-Shaarbaf
Assist. Prof.
University of Nahrain

Munaf A. A. Al-Rmahee
Assist. Lecture
University of Qadisiya

Abstract

This study describes a three-dimensional material nonlinear finite element model suitable for the analysis of high strength reinforced concrete slabs under different states of loading. The twenty-node isoparametric brick element has been used to model the concrete while reinforcing steel bars have been idealized as axial members embedded within the brick elements. The behavior of concrete in compression is simulated by an elasto-plastic work hardening model followed by a perfectly plastic response, which is terminated at the onset of crushing. In tension, a smeared crack model with fixed orthogonal cracks has been used with the inclusion of models for the retained post-cracking tensile stress and for the reduced shear modulus. Three high strength reinforced concrete slabs and one normal strength concrete slab have been analyzed in the present study with different boundary conditions and loading arrangements. Parametric studies have been carried out to investigate the effect of some important finite element and material parameters. These parameters include the compressive strength of concrete, amount of reinforcement and slab thickness. The finite element analysis indicated that when the concrete compressive strength of the slab is increased from (35 MPa) to (80 MPa) an increase in the ultimate capacity of about (60%) has been achieved. In general good agreement between the finite element solutions and the available experimental results have been obtained

Keywords: Finite element ; Brick element; High strength concrete slab ; Plasticity models; Compressive strength

التحليل اللاخطي للبلاطات الخرسانية المسلحة عالية المقاومة باستخدام طريقة العناصر المحددة

الدكتور إحسان علي صائب الشعرباف
أستاذ مساعد
جامعه النهرين – كلية الهندسة

مناف عبد المهدي عبد الكاظم الرماحي
مدرس مساعد
جامعه القادسية – كلية الهندسة

الخلاصة

تصف هذه الدراسة أنموذجا لا خطيا ثلاثي الأبعاد بطريقة العناصر المحددة لتحليل البلاطات الخرسانية المسلحة ذات المقاومة العالية تحت تأثير حالات مختلفة من التحميل. تم استخدام العنصر الطابوقي الثلاثي الأبعاد ذي العشرين عقدة لتمثيل الخرسانة.أما حديد التسليح فقد تم تمثيله باستخدام عنصر أحادي البعد (محوري) مطمور في عنصر الخرسانة. تم تمثيل تصرف الخرسانة تحت اجهادات الضغط باستخدام النموذج المرن- اللدن ذو التقوية الانفعالية (Elasto – Plastic Strain Hardening) والمتبوع

بتصرف لدن تام(Perfectly Plastic) يستمر لغاية أقصى انفعال انضغاط تتهشم عنده الخرسانة. أما تحت تأثير اجهادات الشد فقد تم تبني نموذج التشقق المنتشر (Smeared Crack Model) كما تمت الاستعانة بأنموذج يأخذ بنظر الاعتبار اجهادات الشد المتبقية في الخرسانة بعد التشقق وأنموذج لتخفيض قيمة معامل القص (Shear Modulus of Rigidity) بعد حصول التشقق. في هذه الدراسة تم تحليل ثلاثة بلاطات خرسانية مسلحة عالية المقاومة وبلاطة واحدة ذات مقاومة عادية ذات حالات إسناد وتحميل مختلفة.أجريت تجارب عديدة لدراسة تأثير بعض المتغيرات المهمة كتلك المتعلقة بالنمذجة وتمثيل خواص الخرسانة عالية المقاومة، وتلك المرتبطة بطريقة تحليل العناصر المحددة.تضمنت هذه المتغيرات مقاومة الانضغاط للخرسانة، كمية حديد التسليح وسمك البلاطة. بينت النتائج التحليلية بان زيادة مقاومة الانضغاط للخرسانة في البلاطات من (35MPa) إلى (80 MPa) يؤدي إلى زيادة الحمل الأقصى بحوالي (60%). وقد وجد بصورة عامه إن التحليل اللاخطي ثلاثي الأبعاد يعطي توافقا جيدا مع النتائج العملية.

Notation

C_p	Plasticity coefficient
Ec	Modulus of elasticity of concrete
Es	Modulus of elasticity of steel reinforcement
f	Yield function
f'c	Uniaxial compressive strength of concrete
ft	Uniaxial tensile strength of concrete
fy	Yield stress of longitudinal reinforcing bars or stirrups
I_1	First stress invariant
J_2	Second deviatric stress invariant
Ni	Shape function of node i of the brick element
u,v,w	Displacement components in the x,y and z-direction
X,Y,Z	Global coordinate system
v	Poisson's ratio
α_1, α_2	Tension-Stiffening parameters
c	Matreial constant
β	Shear retention factor or material constant
σ_n, σ_c	Stress
σ_o	Effective stress at onset of plastic deformation
σ_{cr}	Cracking stress
ε_n, ε_c	Strain
ε_{cu}	Concrete ultimate strain
ε_o	Strain corresponding to peak uniaxial concrete compressive stress
ε_{cr}	Cracking strain
γ_1, γ_2, γ_3	Shear retention parameters
ϱ	Longitudinal reinforcement ratio
ξ,η, ζ	Local coordinate system

Introduction

The development of concrete technology and practice has led to a changing perception of what is high strength concrete. The term high strength concrete is generally used for concrete with compressive strength higher than 41 MPa (Rasmussen et al.1995).Its use in construction industry has increased steadily in recent years because it results in reduced dead loads, which leads to longer spans and taller structures. However high strength concrete is considered to be a relatively brittle material because the post- peak portion of its strain-stress diagram descends deeply or almost vanishes as the compressive strength increases (Baksh et al.1990). The inverse relationship between strength and ductility is a series drawback in using this material. In spite of the wide use of high strength concrete, little information is available on the structural behavior of this new material. In the last decade, extensive research work has been conducted on the structural behavior of high – strength beams and columns. Little investigations of the structural behavior of two way slabs are available. At present, the finite element technique is considered as the must efficient numerical approach for analyzing reinforced concrete members. This technique has been adopted in this research work to analyze high strength reinforced concrete slabs. In this analysis, the slab is divided into a number of three dimensional brick elements. The behavior of reinforced concrete is governed by many factors, such as the tensile stress redistribution after cracking , crushing of concrete, nonlinear inelastic stress-strain relation for concrete in compression and yielding of steel reinforcement.

Finite Element Model

The twenty-node isoparametric brick element shown in **Figure (1)** is used in the current study to model the concrete. Each node of this element has three degrees of freedom u, v, and w in the x, y, and z directions respectively. The definition of the displacements within the brick element is given by :

$$u(\xi,\eta,\zeta)=\sum_{i=1}^{20} N_i(\xi,\eta,\zeta).u_i$$
$$v(\xi,\eta,\zeta)=\sum_{i=1}^{20} N_i(\xi,\eta,\zeta).v_i \qquad (1)$$
$$w(\xi,\eta,\zeta)=\sum_{i=1}^{20} N_i(\xi,\eta,\zeta).w_i$$

where Ni (ξ, η, ζ) is the shape function at the i-th node and ui, vi, wi are the corresponding nodal displacements. The shape functions for the 20 node brick element which are adopted to map the element are given in **Table(1)**.

The three-dimensional finite element problems require a relatively large amount of computation time because considerable proportion of which is used in the numerical integration in order to setup the elements stiffness matrices. The Gauss-Legender quadrature numerical integration scheme has been found to be accurate and a convenient technique to carry out the finite element analysis. The integration rule, which has been used in this study , is the

twenty seven point rule. Also the (15a), (15b) and 8- point rules are used in this research as a parametric study in order to show the effect of using these rules on the finite element solutions compared with the twenty seven point rule. The corresponding weights and abscissa for the 27-point rule are listed in **Table(2)** and the relative positions of the sampling point over the volume of

Outline of the Computer Program

The computer program 3DNFEA (3-Dimensional Nonlinear Finite Element Analysis) has been used in the present study(Al-Shaarbaf.1990). In the current research work, the computer program has been generalized to deal with high strength concrete as well as normal strength concrete slabs. The main objective of the computer program is to analyze reinforced concrete members under general three-dimensional states of loading up to failure. In the present study ,the computer program had been proceed using **FORTRAN 90**(Power station 4.0) compiler . The program has been implemented on Pentium IV, 1700MHz IBM compatible computer with 256 Megabyte RAM.

Modeling of Material Properties

The material model used in the present work is suitable for the three-dimensional nonlinear analysis of reinforced concrete structures under monotonically increasing load. The behavior of concrete in compression is presented by an elastic-plastic strain hardening model followed by a perfectly plastic response, which is terminated at the initiation of crushing. The growth of subsequent loading surfaces is described by an isotropic hardening rule. A parabolic equivalent uniaxial stress-strain curve shown in **Figure (3)** has been used to represent work hardening stage of behavior and the plastic straining is controlled by an associated flow rule. A yield criterion suitable for analyzing reinforced concrete members has been used. This criterion was used successfully can be expressed as:

$$f(\{\sigma\}) = cI_1[(cI_1)^2 + 3\beta J_2]^{1/2} \qquad (2)$$

where c and β are material parameters to be determined by fitting biaxial test results. Using the uniaxial compression test and the biaxial test under equal compressive stresses. I_1 and J_2 are the first stress and second deviatoric stress invariants and σ_0 is the equivalent effective stress taken from uniaxial tests.

In tension, linear elastic behavior is assumed to occur prior to cracking. Crack initiation is controlled by a maximum tensile stress criterion. A smeared crack model with fixed orthogonal cracks has been adopted to represent the behavior of cracked sampling points. The retained post-cracking tensile stress and the reduced shear modulus are calculated according to **Figure(4)** and **Figure(5)** respectively. Details of the plasticity based model in compression and the smeared crack model in tension can be found elsewhere (Al-Rmahee.2005).

Analysis of High Strength Reinforced Concrete Slabs

In this section, two high strength reinforced concrete slabs have been analyzed using the finite element technique and the models described in the pervious section. The selected slabs are two-way slabs and were simply supported along their four edges at a distance (100mm) from the edges with the corners being free to lift . The selected slabs failed in flexure. The three dimensional nonlinear finite element techniques have been used for the analysis using the computer program **(P3DNFEA)**.The finite element results have been compared with the available experimental data. In the following sections a description of the slabs and the validity of the finite element analysis are presented.

Analysis of High Strength Reinforced Concrete Slab (HS1)

A simply supported two-way high strength reinforced concrete slab designated as HS1 was analyzed to investigate the applicability and accuracy of adopted finite element models. This slab was selected from the experimental tests carried out by Marzouk and Hussein (4) in 1990 .The obtained analytical results have been compared with the results reported in Reference No.4 . The slab is loaded by a concentrated load through a column stub at the center of the slab. The dimensions and reinforcement details are shown in **Figure (6).** Material properties of the analyzed high strength slab are listed in **Table(3)**. By taking advantage of symmetry, a segment representing one-quarter of slab was taken in the finite element modeling. This segment was divided into (149) brick elements. Another finite element mesh has also been used to asses the accuracy of the finite element model. These mesh consisted of (100) brick elements, **Figure (7)**.

Results of Analysis

The analytical load –mid span deflection curves obtained for the two meshes considered are compared with the available experimental data as shown in **Figure (8)** .From this figure it can be noted that the finite element solutions are in good agreement with the experimental results for both meshes throughout the entire range of loading. The results obtained using the mesh with (149) elements are closer to the experimental results compared with those obtained using the mesh of (100) elements. It can be observed that for the analytical curve obtained for the first mesh (149 elements), the ultimate load was (175) kN (1.7 % less than the experimental ultimate load). The deflection at ultimate load was (25.7)mm (1.01% greater than the corresponding experimental value). For the second mesh(100 elements), the ultimate load was (188) kN (1.056% greater than experimental ultimate load). The deflection at ultimate load was (25.5)mm (1.001% greater than the corresponding experimental value).

Figure (9) shows the stress distribution along a typical middle steel bar and a steel bar located at edges of the slab obtained from finite element analysis at the last converged increment of loading. it can be shown that a maximum tensile stress of (385 MPa) occurred at the center of the middle bar. It was also observed that small stresses occurred at region located at the support.

Analysis of High Strength Reinforced Concrete Slab.HS11

A simply supported two-way high strength reinforced concrete slab was analyzed to investigate the validity and accuracy of the adopted finite element models. This slab (designated as HS11) was also chosen from the experimental tests carried out by Marzouk and Hussein (4) .The analysis results obtained have been compared with the available experimental data. This slab differed from slab HS1 in its thickness, reinforcement ratio and concrete compressive strength. The obtained analytical results have been compared with the experimental results reported in Reference No.(4). The slab is loaded by a concentrated load through a column stub at the center of slab. Dimensions and reinforcement details of the slab are shown in **Figure (9)**. Material properties of the analyzed high strength slab are listed in **Table (4)**. The selected quarter of the slab was discritized into (100) finite elements with two elements through the slab thickness. A second finite element mesh was used to study the accuracy of the finite element model. The second mesh consisted of (50) brick elements with one element through the slab thickness, **Figure (10).**

Results of Analysis

Figure(11) represents the analytical load-deflection curves compared with the experimental load-deflection curve for the two used meshes. From this figure, it is observed that the finite element response is in good agreement with the experimental results up to a load level of (80) kN. After this stage of loading a relatively stiffer analytical response is obtained up to (144) kN. It can be shown that the results obtained using the mesh of (100 elements) are closer to the experimental result compared with these obtained using the mesh of (50 elements).The predicated ultimate load obtained using the mesh of (100 elements) was (195) kN (0.6 % less than the experimental ultimate load). The deflection at ultimate load level was (27.4)mm (1.014% greater than the corresponding experimental value). For the mesh of (50 elements) the ultimate load was (205) kN (1.045% greater than the experimental ultimate load) and the deflection at ultimate load level was (26.054) mm (3.6%less than the corresponding experimental deflection). Also **Figure (12)** shows the stress distribution along a typical middle steel bar obtained from finite element analysis at the last converged increment of loading . It can be shown that a maximum tensile stress of (512.5MPa) occurred at the center of the middle bar. It was also observed that small compressive stresses occurred at region located at the support.

Parametric Study

In this section, selected slabs were analyzed to investigate the effect of some important material and solution parameters on the numerical load deflection response and ultimate capacity. The investigations considered in the study include the effect of grade of concrete, amount of reinforcing steel and slab thickness. The parameters related to the finite element solutions are the tension stiffening model, integration rule and convergence criteria. The

parametric studies are based on the models and techniques described in the previous sections. The finite element analyses presented in this section have been generally carried out by considering material nonlinearities. The modified Newton – Raphson solution techniques has been used with a work done convergence criterion having a tolerance of 3%.

Effect of Grade of Concrete

The two high strength reinforced concrete slabs tested by Marzouk and the normal strength reinforced concrete slab, which have been described in the previous section, are used to study the influence of the grade of concrete on the behavior and ultimate loads. It was found that the behavior of the slabs with low compressive strength of concrete is softer than those of concrete having higher strengths. The analysis result indicates that an increase in the compressive strength by about 10 % leads to an increase in the ultimate load by about 4 %. **Figures (13)** and **(14)** show the response of the considered high strength reinforced concretes slabs for different concrete compressive strength. **Figures (15)** and **(16)** show the effect of the compressive strength of concrete on the stress distribution of a typical middle steel bar of the high Strength Reinforced Concrete Slab (HS1) and the (HS11). It can be shown that an increase in the value of compressive strength by (25%) leads to a decrease in the maximum tensile stress in steel by about (18%), while by decreasing the compressive strength by (25%) leads to an increase in tensile

Effect of Slab Thickness

To study the influence of using different slab thickness on the behavior of high strength reinforced concrete slabs, slab (HS11) was reanalyzed with three different values of thickness. The selected values were (45), (90) and (135) mm. The load – deflection curves obtained from the finite element analysis together with the experimental test results (slab thickness 90 mm) are shown in **Figure (17)**. The finite element results reveal that a considerable increase in the ultimate load capacity has been achieved by increasing the slab thickness. The ultimate load obtained for thicknesses of (45), (90) and (135) mm are (160), (195) and (225) kN respectively. It can be noted that an increase in the slab thickness of 50% leads to an increase the ultimate load by about 15% while decreasing the thickness to 50% leads to a decrease in the ultimate load by about 18%.

Effect of Amount of Reinforcement:

Figure (18) shows the effect of using of different amounts of reinforcement on the load-deflection behavior of slab (HS1) .Four different steel ratios were used for the finite element analysis. Obviously, a stiffer analytical response was noticed for with high amount of steel. It can be noted that the deflection of the slab at ultimate load was decreased with increasing the amount of steel. The finite element analysis indicated that the ultimate capacity is increased by about (25%) when the steel ratio is increased by (50%). **Figure (19)** shows the profile

of steel stresses along the length of a typical steel bar located at the mid-span of slab (HS1) for different steel ratios. It is shown that the steel stresses dropped sharply with the distance from the slab center.

Effect of Integration Rule

The influence of using different integration rules on the load deflection curve of slab (HS11) are shown in Fig. (20). The slab has been analyzed using the 27, 15a, 15b and 8 point rules. The predicted load-deflection curves are generally in good agreement with the experimental results. The 27-point integration rule resulted in a predicted response closer to the experimental behavior. This can be attributed to the relative distribution of sampling points within the brick element. A relatively stiffer response has been obtained for the 8- point rule while a softer behavior has been obtained using the 15 a and 15 b rules. The CPU time recorded at the end of the last converged increment of loading were (8.12), (16.26), (14.39) and (30.41) minutes for the 8, 15a, 15b and 27-point rules respectively. Therefore, the 27-point has been used for all analysis considered in the current research work.

Summary and Conclusions

A nonlinear finite element analysis of high strength reinforced concrete slabs using a full three dimensional model have been presented. The main objectives of this study are to investigate the accuracy and efficiency of the computational finite element models in simulating the structural behavior of structures. The adopted material constitutive relationships are based on the incremental theory of plasticity of concrete in compression and the smeared crack representation of concrete in tension with an elastic-linear work hardening model used to simulate the behavior of reinforcement. Several parametric studies have been carried out in the current research to investigate the effect of some material and numerical parameters on the predicted behavior of the high strength reinforced concrete slabs.

Based on the finite element analysis carried out throughout the present work, the following conclusions are drawn:

1. The three – dimensional finite element model used in the present research work is capable to simulate the behavior of high strength reinforced concrete slabs. The finite element solutions obtained for different slabs are in good agreement
with the corresponding experimental results.

2. The finite element analysis indicated that when the concrete compressive strength of the slab is increased from (35 MPa) to (80 MPa) an increase in the ultimate capacity of about (60%) has been achieved.

3.The finite element analysis indicated that the increase in the compressive strength of concrete from (67MPa) to (80MPa) leads to a decrease in the maximum tensile stress in steel by about (18%).While when the compressive strength of concrete decreases from (67MPa) to (52.5MPa) an increase in tensile stress in steel by about (15%) is obtained .

4. The finite element solutions reveal that the ultimate load of the considered slabs increases with the increase of the amount of reinforcement, when the steel ratio is increased by about (50%) an increase in the ultimate load capacity by (25%) is achieved.
5. According to finite element analyses conducted in this work , it is found that by increasing the slab thickness from (90mm) to (135mm) a considerable increase in the ultimate load capacity about of (15%) is obtained. Also by decreasing the thickness of slab from (90mm) to (45mm) a decrease in ultimate load capacity of slab by (18%) is achieved.
6. Throughout this research work, the (27), (15a), (15b) and (8) point integration rules have been used. The load deflection behavior obtained using the 27-point integration rule has been compared with those obtained by using (15a), (15b) and (8) point rules. The finite element solutions reveal that the results of the 27- point rule are closer to experimental data compared with the results of the other rules. The (CPU) time recorded for the (15a), (15b) and (8) integration rule was less than recorded for the (27) integration rule by (70%), (40%) and (44%) respectively.

References

1- Rasmussen, L.J. and Baker, G. "Torsion in Reinforced Normal and High Strength Concrete-part 1 : Experimental Test Series" ACI Journal, 1995, pp.149-155.
2- Baksh, A.H., Wafa,F. and Akhtaruzzaman,A.," Torsion Behavior of Plain High Strength Concrete Beams" ACI-Structural Journal,1990,pp.583-588.
3- Al-Shaarbaf, I.A.S., "Three-Dimensional Nonlinear Finite Element Analysis of Reinforcement Concrete Beams in Torsion" PhD Thesis. University of Bradford, 1990. pp.323
4- Marzouk .H. and Hussein, A. Experimental Investigation on the Behavior of High – Strength Concrete Slabs. ACl. Structural Journal, Vol. 88.No.6, 1991, pp.701-713.
5- Al-Saidi, B.A.S. "Nonlinear Finite Element Analysis of Reinforced Concrete Slabs" M.Sc. Thesis .University of Al-Nahrain, 2003.pp124.
6- Al-Rmahee, M.A.A "Nonlinear Finite Element Analysis of High Strength Reinforced Concrete Slabs" M.Sc. Thesis. University of Kufa, 2005. Pp111.

Table (1): Shape functions of the twenty-node isoparametric element

Location	ξ_i	η_i	ζ_i	$N_i(\xi_i, \eta_i, \zeta_i)$
Corners nodes	±1	±1	±1	$0.125(1+\xi\xi_i)(1+\eta\eta_i)(\xi\xi_i+\eta\eta_i+\zeta\zeta_i-2)$
Mid-side nodes	0	±1	±1	$0.25(1-\xi^2)(1+\eta\eta_i)(1+\zeta\zeta_i)$
Mid-side nodes	±1	0	±1	$0.25(1+\xi\xi_i)(1-\eta^2)(1+\zeta\zeta_i)$
Mid-side nodes	±1	±1	0	$0.25(1+\xi\xi_i)(1+\eta\eta_i)(1-\zeta^2)$

Table (2): Weight and abscissa of sampling points used in this study

Integration rule	Sampling point number	ξ	η	ζ	Weight
27(3*3*3)	1,3,5,7,19,21,23,25	± 0.7746	± 0.7746	± 0.7746	0.171468
	2,6,20,24	± 0.7746	0	± 0.7746	0.2743
	4,8,22,26	± 0.7746	± 0.7746	0	0.2743
	10,12,14,16	0	± 0.7746	± 0.7746	0.2743
	13,17	0	± 0.7746	0	0.43895
	9,27	± 0.7746	0	0	0.43895
	11,15	0	0	± 0.7746	0.43895
	18	0	0	0	0.70233

Table (3): Material properties and finite element parameters used for slab, HS1.

CONCRETE SPECIFICATION	
Compressive strength, *f*`c(MPa)	**67**
Young's Modulus, Ec (GPa)	**38.47**
Tensile strength , f_t (MPa)	**6.7**
Poisson's ratio ,ν*	**0.20**
Uniaxial crushing strain ,ε_{cu}	**0.0025**
STEEL SPECIFICATION	
Young's Modulus , Es(GPa)	**190**
Yield stress *f*y (MPa)	**496**
Hardening parameter +, H	**12.66**
Poisson's ratio ,ν*	**0.25**

$f_t=0.1f\grave{c}$; $^{+}H=Es/15$; $Ec=4700(f\acute{c})^{0.5}$; $\varepsilon_{cu}=(4.0-f\acute{c}/45)^{*}10^{-3}$

Table (4) Material properties and finite element parameters used for Slab,HS11 .

CONCRETE SPECIFICATION	
Compressive strength, $f`c$(MPa)	**70**
Young's Modulus, Ec (GPa)	**39.323**
Tensile strength , f_t (MPa)	**7.0**
Poisson's ratio ,v^*	**0.20**
Uniaxial crushing strain ,ε_{cu}	**0.004**
STEEL SPECIFICATION	
Young's Modulus , Es(GPa)	**190**
Yield stress fy (MPa)	**496**
Hardening parameter $^+$, H	**12.66**
Poisson's ratio ,v^*	**0.25**

ft=0.1fc̀ ;$^+$H=Es/15$^{(73)}$; Ec=4700(fć)$^{0.5}$; ε_{cu}=(4.0-fć/45)

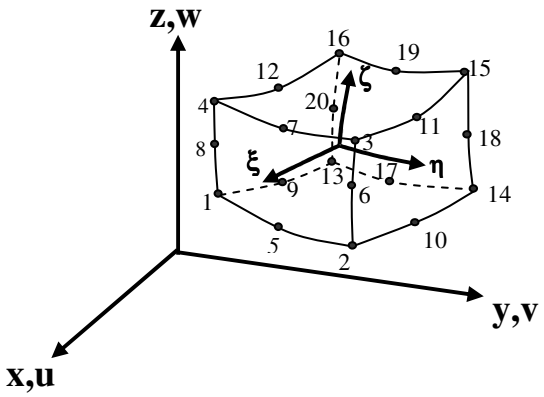

Figure. (1): Twenty-node brick element

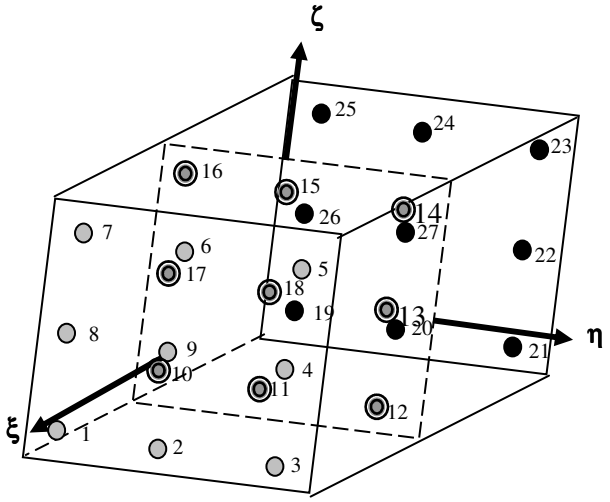

Figure (2) Distribution of the sampling points

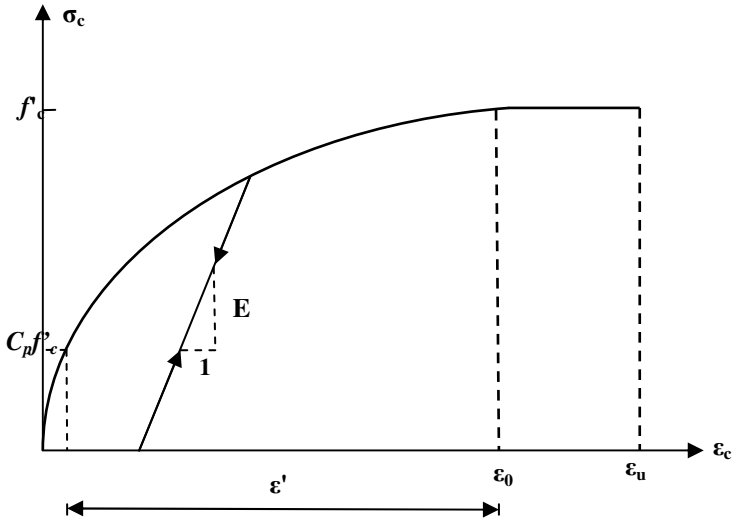

Figure (3): Uniaxial stress-strain curve for concrete in compression.

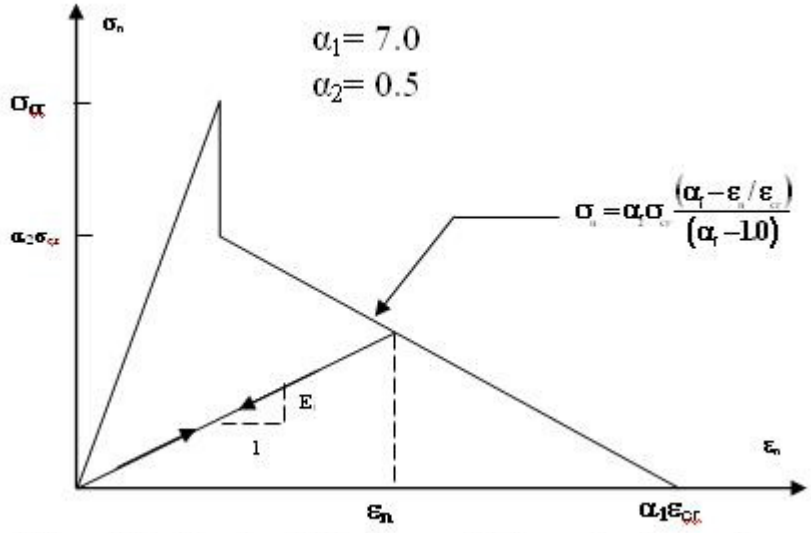

Figure (4): Tension-stiffening model for cracked concrete.

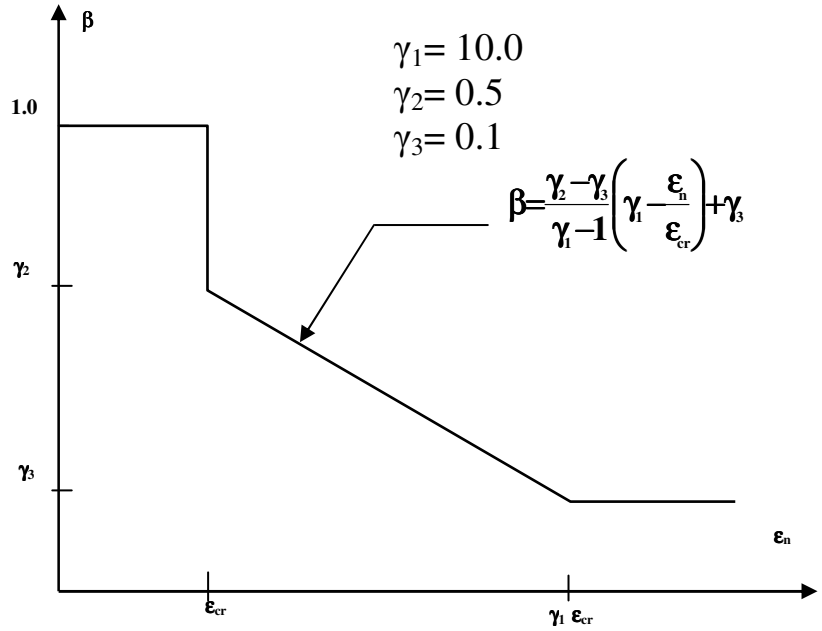

Figure (5): Shear retention model for cracked concrete.

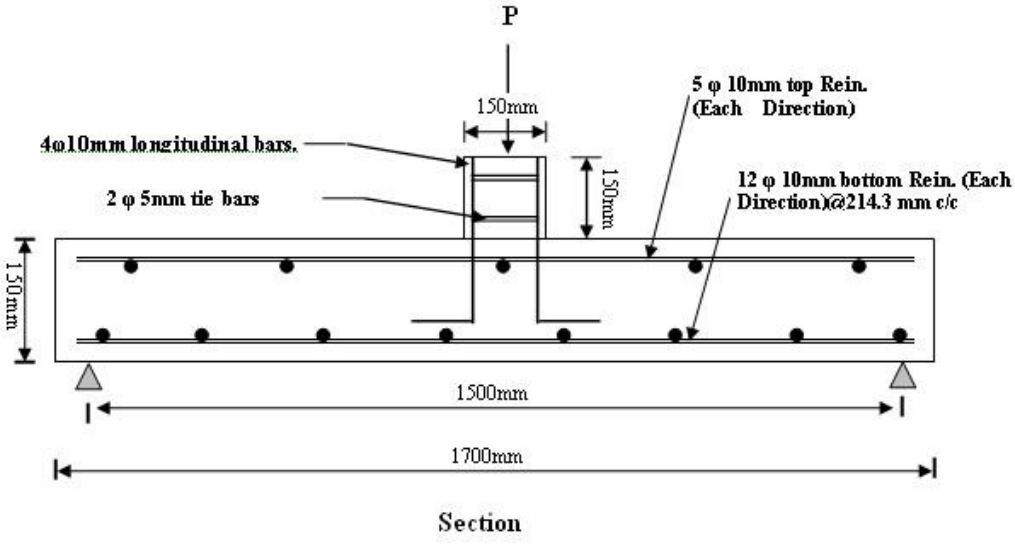

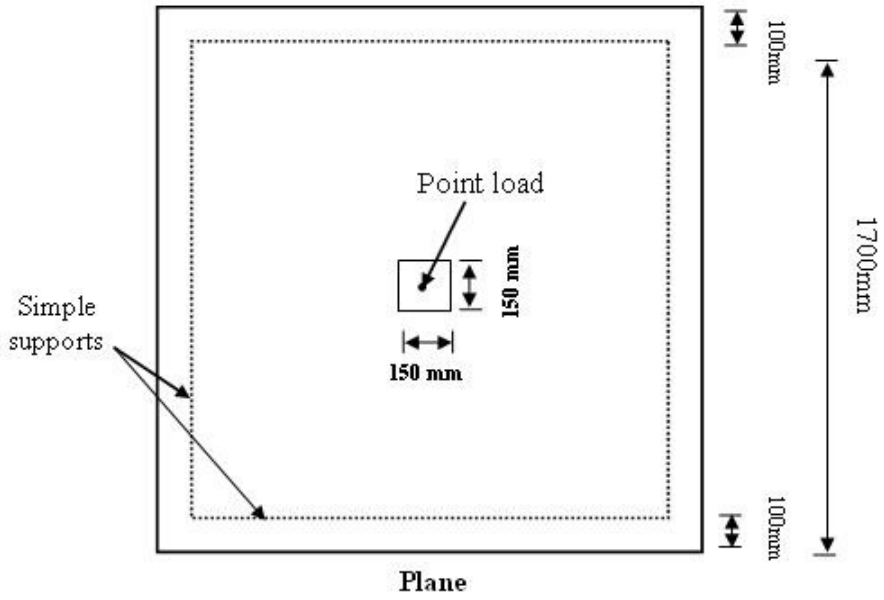

Figure (6): Geometry, boundary conditions, loading arrangement and reinforcement details of slab HS1

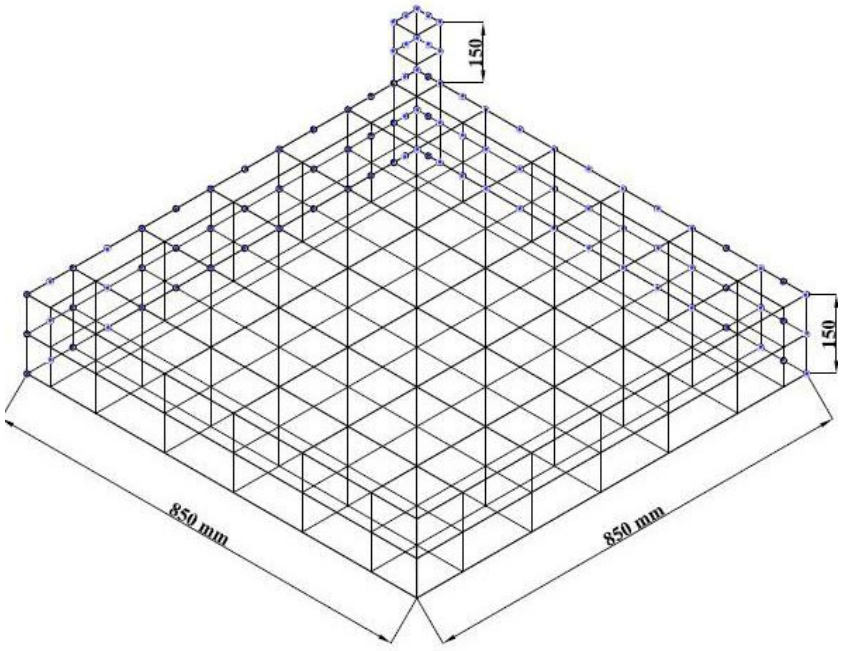

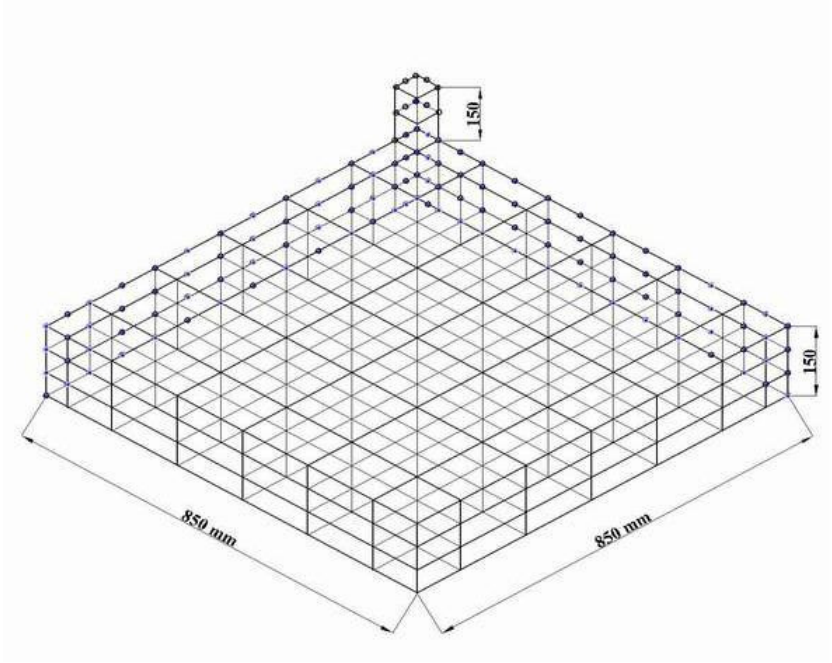

Figure (7) Finite element meshes used for slab, HS1

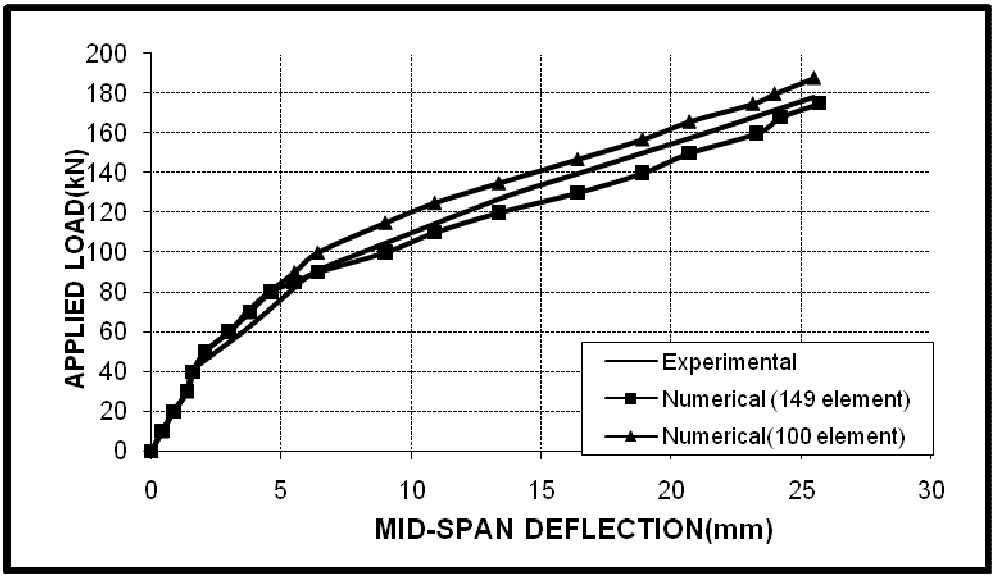

Figure.(8) Load-deflection behaviour of slab, (HS1)

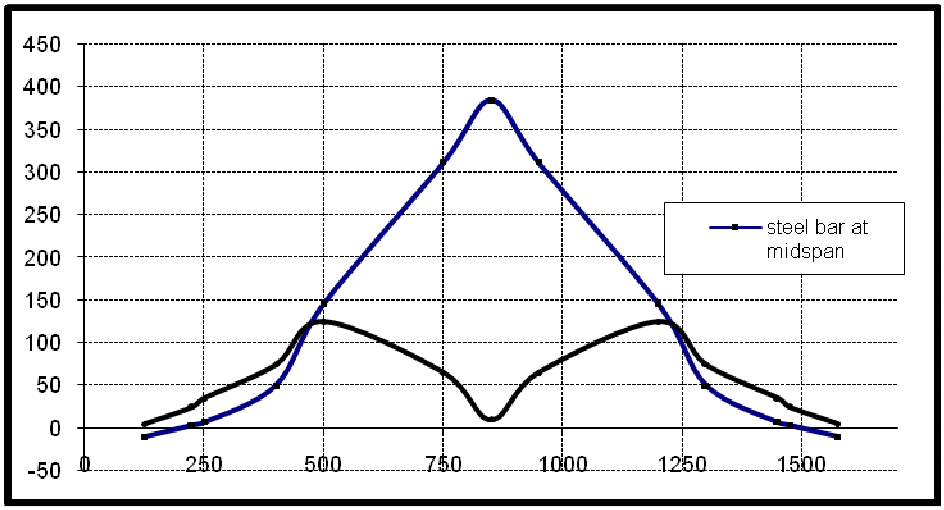

Figure (9) Slab HS1, stress distribution in steel bar at load level (178 kN)

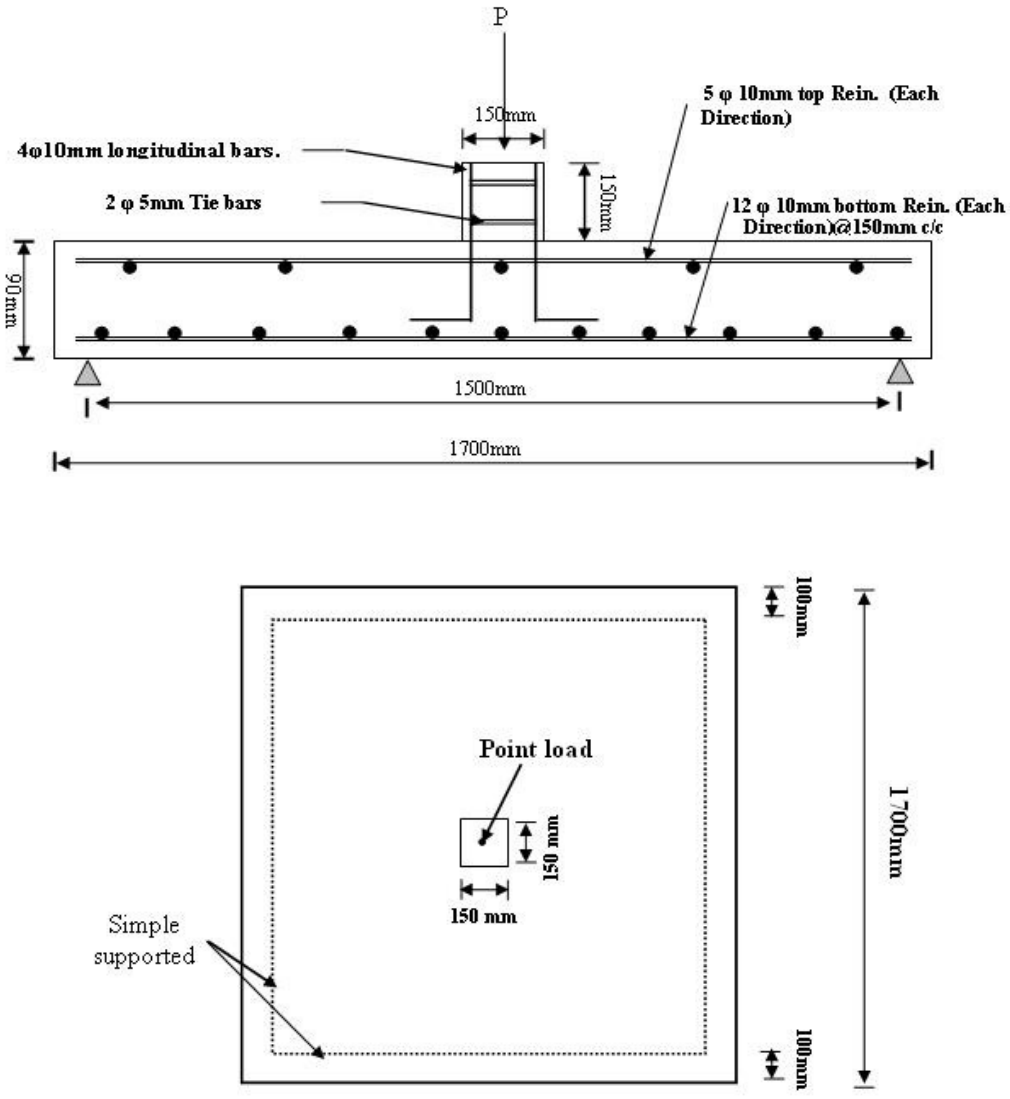

Figure (9) Geometry, boundary conditions, loading arrangement and reinforcement details of slab HS11

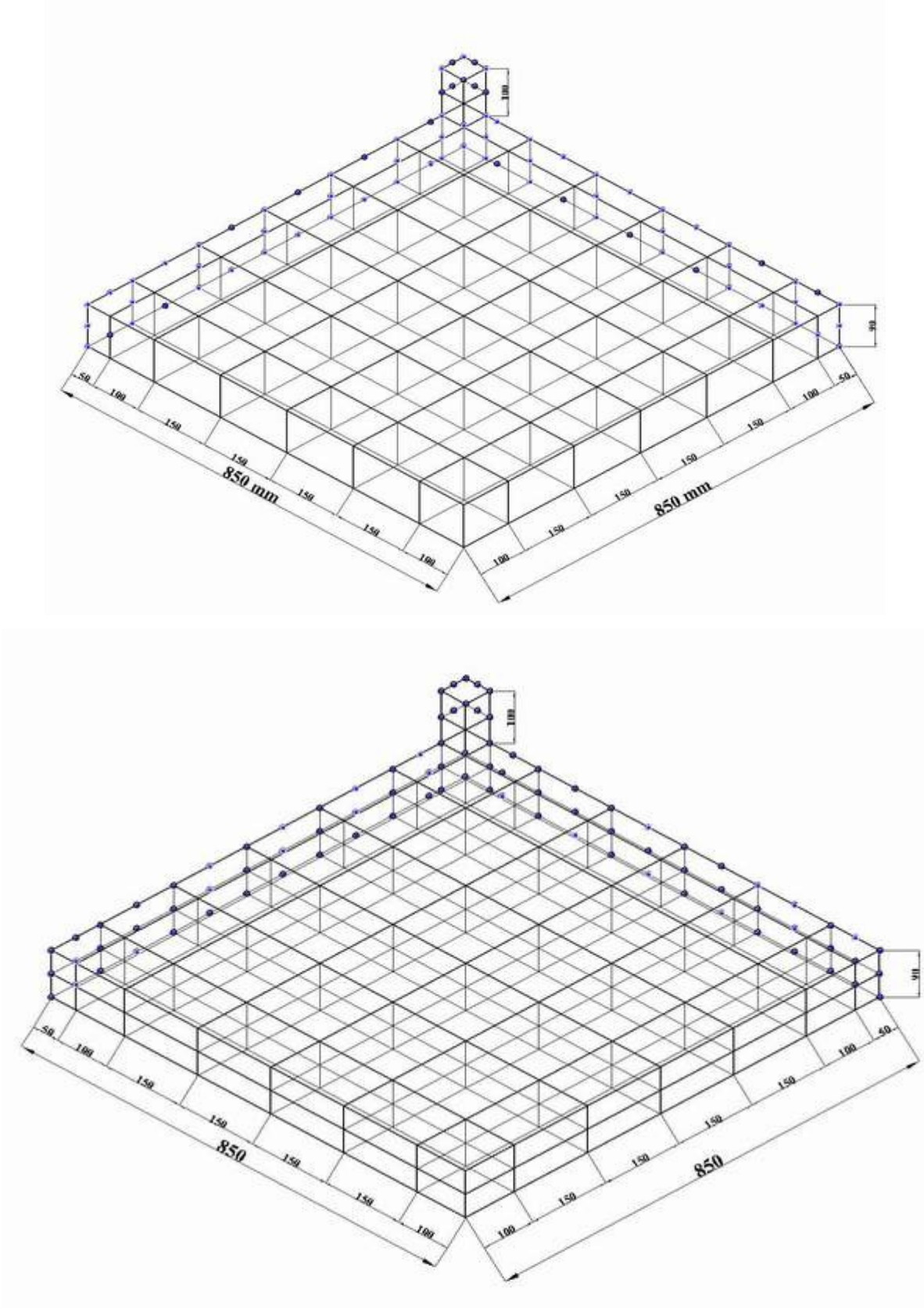

Figure (10) Finite element meshes used for slab, HS11

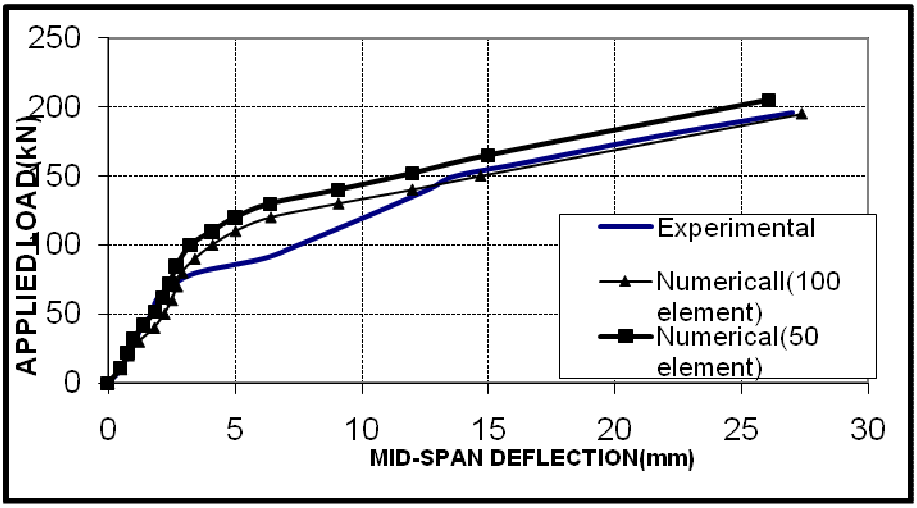

Figure (11)Load-Deflection Behaviour of Slab (HS11)

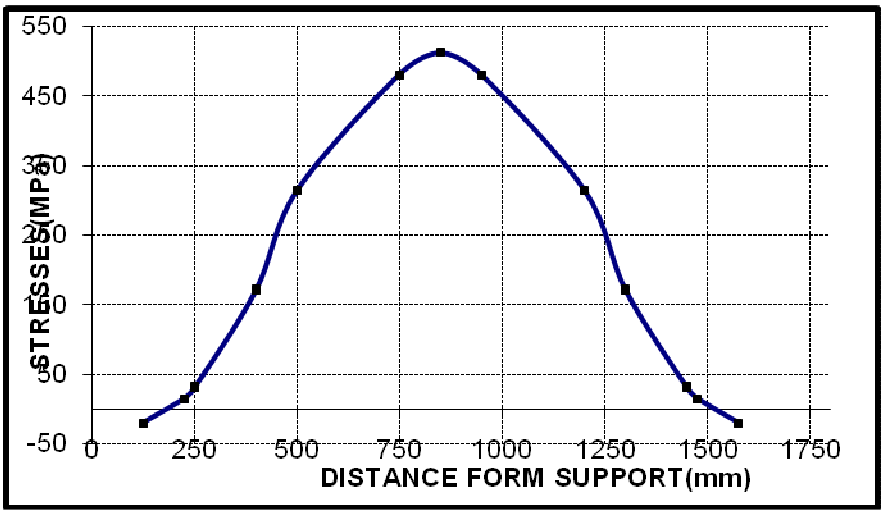

Figure (12) Slab HS11, stress distribution in the middle steel bar at load level (198 kN)

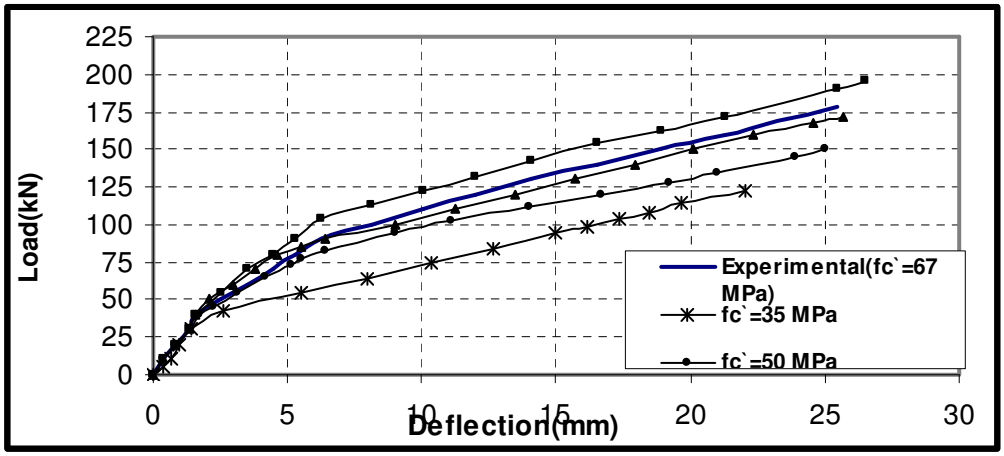

Figure (13) Effect of concrete compressive strength on the load- deflection behavior of slab HS 1

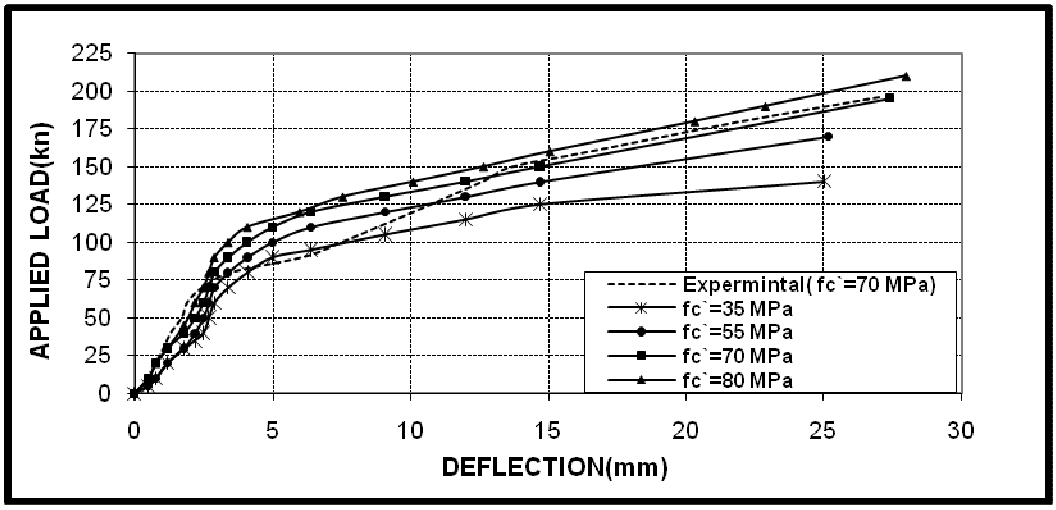

Figure (14) Effect of concrete compressive strength on the load-deflection behavior of slab HS 11

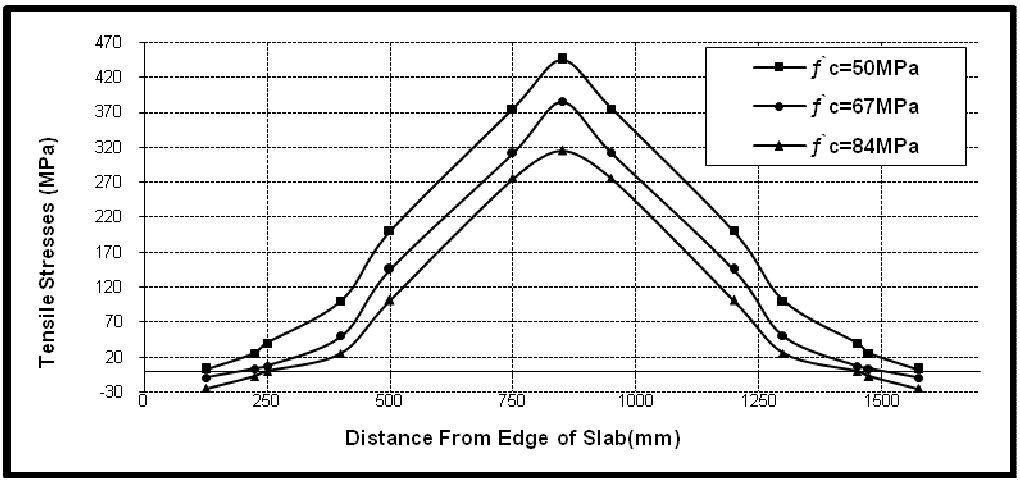

Figure (15) Slab HS1, effect of concrete compressive strength on the stress distribution of a middle steel bar

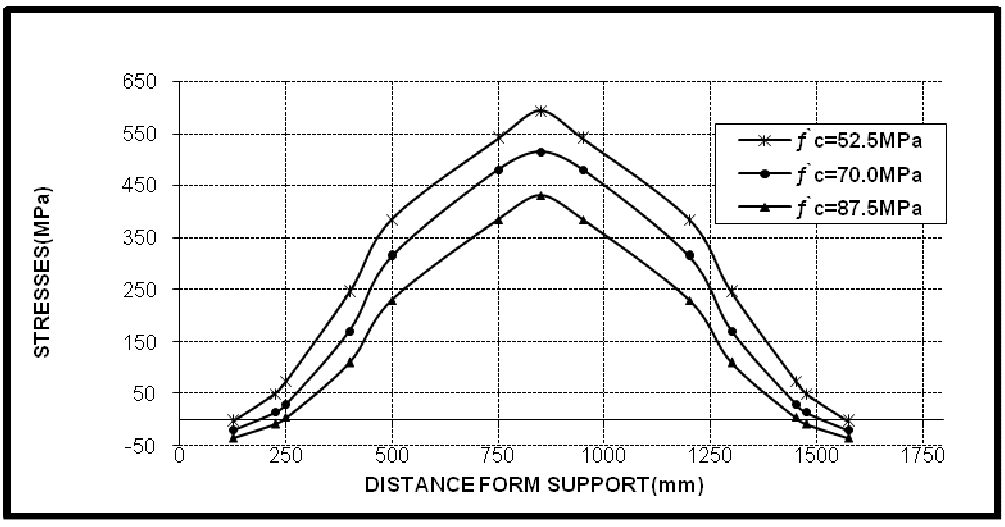

Figure (16) Slab HS11, effect of concrete compressive strength on the stress distribution of a middle steel bar

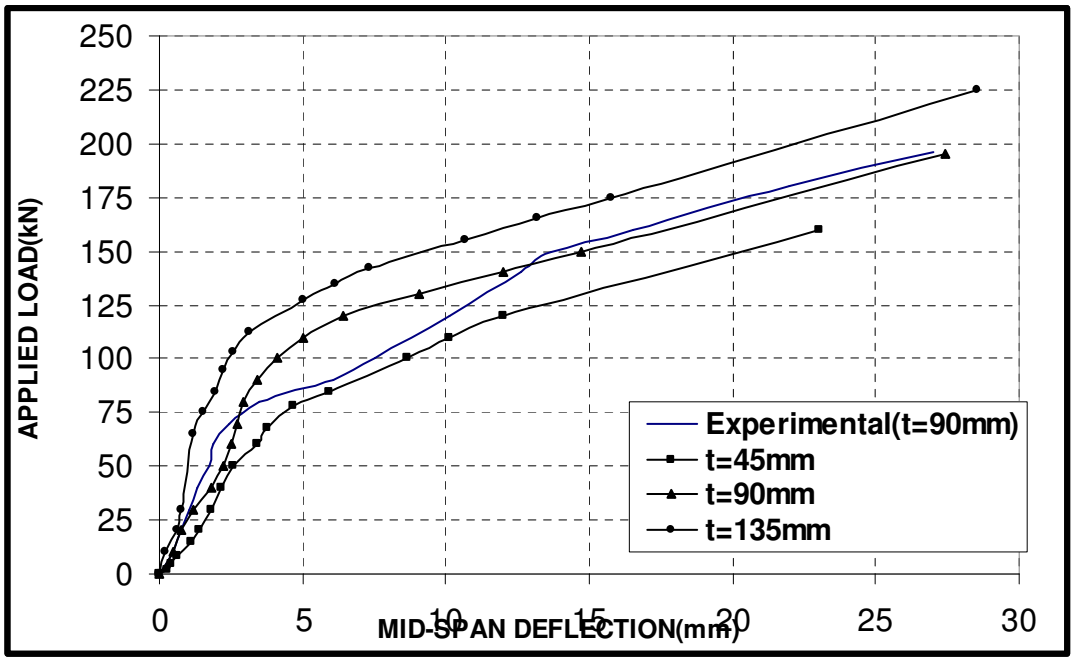

Figure (17) Effect of thickness of slab on the load-deflection curve of slab HS11

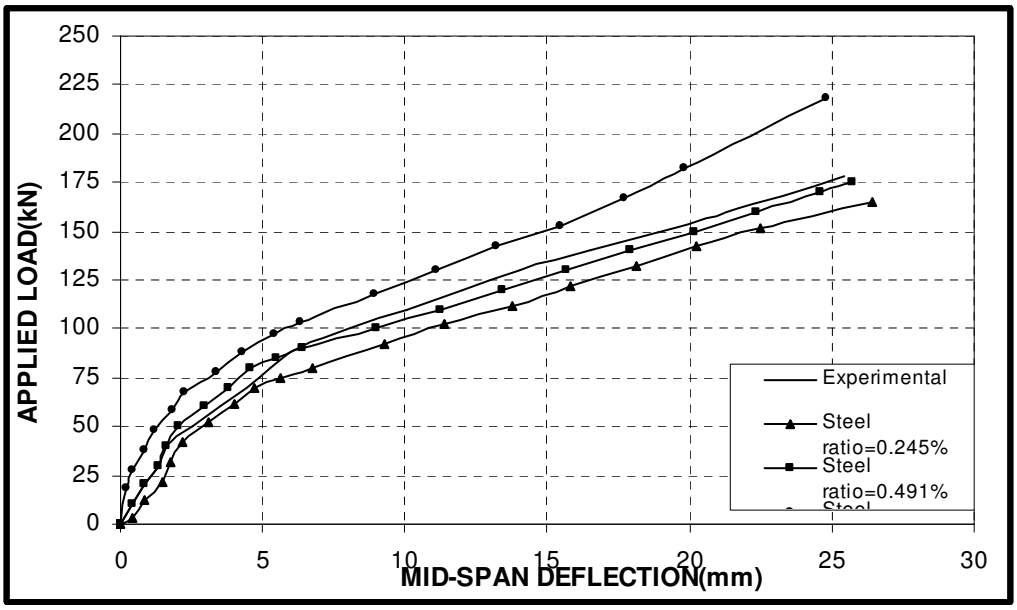

Figure (18) Effect of amount of reinforcement steel on the load –deflection behavior of slab HS1.

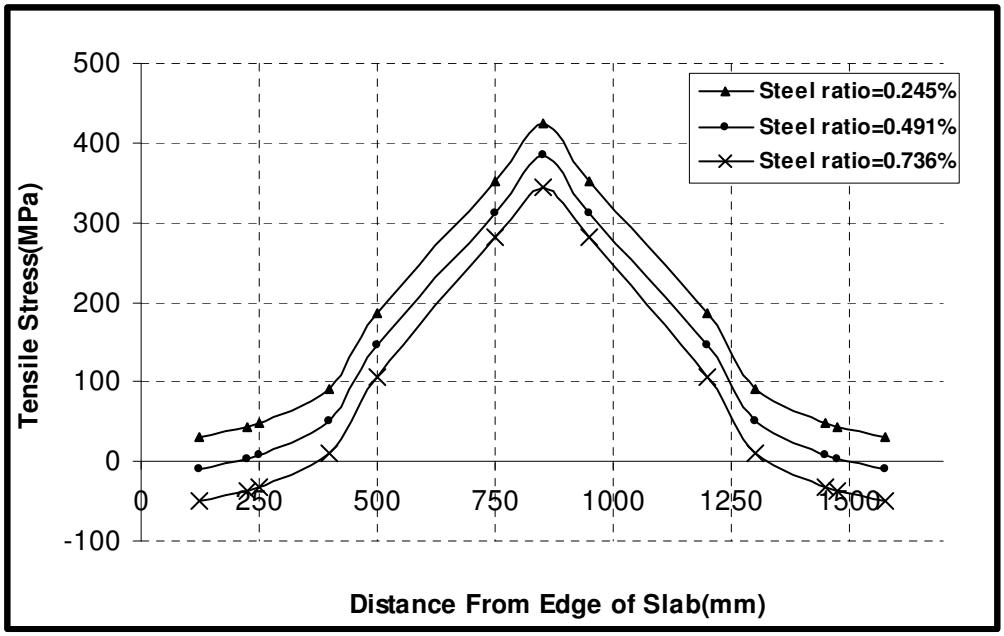

Figure (19) Slab (HS1), Stress distribution along a typical middle steel bar

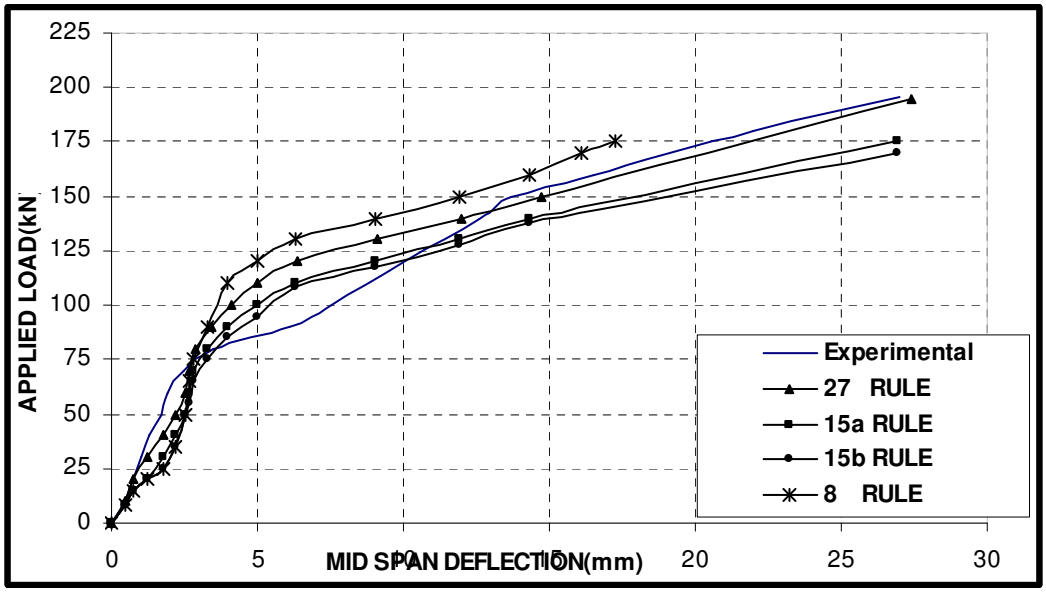

Figure (20) Effect of integration rule on the load-deflection behavior of slab HS11